

## **Punching shear analysis of reinforced concrete flat plates**

Osman M. Ramadan<sup>1)</sup> \*Kamal G. Metwally<sup>2)</sup> and Gehad S. Younis<sup>3)</sup>

<sup>1), 3)</sup> *Department of Structural Engineering, Cairo University, Cairo, Egypt*

<sup>2)</sup> *Department of Civil Engineering, Beni-Suef University, Beni-Suef, Egypt*

<sup>1)</sup> [omoramadan@yahoo.ca](mailto:omoramadan@yahoo.ca)

<sup>2)</sup> [kghamery@gmail.com](mailto:kghamery@gmail.com)

### **ABSTRACT**

This paper presents the results of nonlinear finite element analyses of reinforced concrete slab-column connections. Model verification has been done by simulating experimental data results of another researcher before doing parametric study. A series of finite element models is developed in order to perform a parametric study on interior, edge, and corner slab-column connections. The parametric study investigates the effect of concrete compressive strength, load eccentricity to slab thickness ratio ( $e/t_s$ ), and column dimensions to slab thickness ratio ( $b/t_s$ ) on the behavior of the slab-column connections. Using the proposed finite element model, the punching shear behavior of slab-column connections is shown to be adequately simulated. Punching shear resistance of various slab-column connections is calculated and compared with the corresponding predictions of different design specifications such as: ACI 318-05, CEBFIP MC 90, and BS 8110-97.

### **1. INTRODUCTION**

Reinforced concrete flat plate is commonly adopted as a floor system due to its simple reinforcement layout, fast construction, smaller overall height, and architectural flexibility (no restriction on wall locations). However, the problem of punching shear, which is a brittle failure, is of major concerns in the design of flat plate floors. Punching shear failure could occur as a result of shear stress produced by transfer of shear forces and unbalanced moments. Such shear stresses increase the likelihood of punching failure of slabs, particularly when high moment transfer occurs, as in earthquake load combinations. This study analyzes the behavior of interior, edge, and corner reinforced concrete slab-column connections. Furthermore, relevant experimental and analytical studies are presented. A parametric study using an

---

<sup>1)</sup> Professor

<sup>2)</sup> Ph.D.

<sup>3)</sup> Graduate Student

appropriate finite element model (FEM) of slab-column connections is conducted.

It is generally known that reinforced concrete slab-column connections, when subjected to vertical loads, would produce shear stresses within the slab. These shear stresses are mainly resisted by either adding certain reinforcement layout, or by considering relatively higher slab and/or column stiffness.

It worth mention that the available experimental work concerned on the punching shear of column-slab connection considering various key design parameters such as: the shear reinforcement, concrete compressive strength, yield strength of rebar, thickness of flat slab.

On the other hand, a limited number of analytical work is done using self-developed programs, commercial software, or by utilizing mathematical model. In this paper, the effect of different parameters such as concrete compressive strength, loading eccentricity and column dimensions is studied. This paper presents an overview of the available experimental and analytical literature, in addition to code provisions concerning the behavior of slab-column connections.

In the upcoming part, some models are listed, representing different approaches and conclusions for the punching shear of flat slabs that were made by researchers. Megally and Ghali (2000) illustrated a nonlinear finite element model of both interior and edge column-slab connections. The numerical results indicated that the developed model provided good results of both the ultimate capacity and deformations of column-slab connections failed by punching shear. In addition, the analyses showed that the variations in mesh size and the locations of supports did not affect the results of the analyzed slabs. Moreover, Mufti and Hassan (2005) performed finite element analysis based on the Anatech Concrete Analysis Program (ANACAP). One-half of the bridge deck slabs was modeled using 20-node brick elements. The slab thickness was divided into three layers. In addition, the reinforcement bars were modeled as individual sub-elements within the concrete elements. The stiffness of the rebar sub-elements was superimposed to the concrete element stiffness, in which the rebar resides. They examined the applicability of nonlinear finite element formulation of restrained concrete bridge decks. The accuracy of the nonlinear finite element analysis is demonstrated using test results conducted by other researchers. The results of the finite element analysis are also compared with those obtained from a rational model. The experimental results and the theoretical model provide insight to the fundamental behavior of concrete bridge decks.

On the other hand, Polak (2005) presented a non-linear finite element formulation that assumes a 3D state of stress and strain within each layer of a shell element. Such research indicated that the formulation of shear modulus of cracked concrete cannot be ignored in the layered shell finite element in order to predict the punching load levels properly. Excessively large values of cracked shear modulus will result in over-predictions of shear capacity and thus, in predicting flexural failure instead of punching. The adopted cracked shear modulus value has little influence on the predicted deflections. Also, modeling of dowel action has an impact on both deflections and predicted failure loads.

Furthermore, Hong-Gun Park et al. (2007) discussed the exterior slab column connection subjected to the unbalanced moment developed from the gravity load as well as the lateral load in nonlinear analysis method. It is concluded that the exterior

connection is more susceptible to punching shear failure. Kyoung-Kyu Choi et al. (2007) proposed a new alternative design method and fuzzy based design charts for the accurate prediction of punching shear strength of simply supported interior slab-column connection. In addition, Wenyuan Wang et al. (2008) presented a nonlinear analysis of flat slab model with layered shell element, and identify the influence of the distribution of transverse shear strain on the punching shear failure. Later on, Hong Guan (2009) applied the non-linear Layered Finite Element Method (LFEM). In accordance to such research, the LFEM is an effective tool in global analysis and suitable for the design of reinforced concrete slab-column systems with the aim of achieving optimum structural performance. Also, this study illustrated the influence of the opening on the ultimate strength, which is small when the size of opening is up to 80% of the column size. In addition, increasing the size and aspect ratio (in both x and y-directions) of an opening in the vicinity of the front column face slightly decreases the ultimate shear strength of the connection when the opening size is up to 80% of the column size. Finally, the empirical punching shear strength predictions recommended by ACI 318 are overly conservative. In the same year, Miguel Fernandez Ruiz et al. (2009) formed a new critical shear crack theory based on physical model and overcome most limitations of current codes of practice. Also, Thomas H-K. Kang et al. (2009) implemented a limit state model based on gravity shear ratio and lateral inter story drift for punching shear failure.

Most design codes base their verifications on a critical section, with the punching shear strength of slabs with or/and without shear reinforcement defined as a function of the concrete compressive strength and often of the reinforcement ratio. On the other hand, some codes, such as: ACI 318-05, CEBFIP MC 90, and BS 8110-97, represent different approaches and equations for the punching shear of flat plates are listed hereinafter.

The American Code ACI 318-08 design equation is:

$$v_u < \phi v_c \quad (1)$$

Where:

$v_u$  is the shear stress due to factored loads

$v_c$  is the concrete shear stress resistance

$\phi$  is the safety factor

The critical section is located at  $d/2$  from the face of the column or loaded area. The shear stress obtained at location  $d/2$  is independent from column dimension to effective depth ratio  $c/d$ . The concrete shear resistance equation is limited by the least value of the following three equations (S.I. units):

$$v_c = \left( 2 + \frac{4}{\beta_c} \right) \frac{\sqrt{f'_c}}{12} \quad (2)$$

Where:

$\beta_c$  is the ratio of long side to short side of column, concentrated area or reaction area to

be taken  $\geq 2$ . When  $\beta_c$  is larger than 2, the shear strength tends to  $0.33\sqrt{f'_c}$  which is unconservative. According to ACI-ASCE Committee 426 (1974) the actual shear stress varies from a maximum of  $0.33\sqrt{f'_c}$  around the corners of the column, down to  $0.167\sqrt{f'_c}$  or less along the long sides between the two end sections.

$$v_c = \left( \frac{\alpha_s d}{b_0} + 2 \right) \frac{\sqrt{f'_c}}{12} \quad (3)$$

Where:

$\alpha_s$  equals 40 for interior columns, 30 for edge columns, and 20 for corner columns.

$$v_c = \frac{\sqrt{f'_c}}{3} \quad (4)$$

On the other hand, The Canadian Code CSA A23.3-04 design equation is:

$$v_f < v_r \quad (5)$$

Where:

$v_f$  is the shear stress due to factored loads

$v_r$  is the factored shear stress resistance

Pertaining the allocation of critical sections, the Canadian Code is very similar to the American one. The critical section is taken at a distance equals  $d/2$  from the face of the column or the loaded area. The applied shear stress can be calculated as discussed in the American one. The difference is in the concrete shear resistance equation, which is limited by the least value of the following equations (S.I. units):

$$v_c = \left( 1 + \frac{2}{\beta_c} \right) 0.2 \lambda \phi_c \sqrt{f'_c} \quad (6)$$

Where:

$\beta_c$  is the ratio of long side to short side of column to be taken  $\geq 2$

$\lambda$  is the concrete density factor (1 for normal weight and 0.85 for semi-light weight)

$\phi_c$  is the concrete safety factor (0.6)

$$v_c = \left( \frac{\alpha_s d}{b_0} + 0.2 \right) \lambda \phi_c \sqrt{f'_c} \quad (7)$$

Where:

$\alpha_s$  is the 4 for interior columns

$\alpha_s$  is the 3 for edge columns

$\alpha_s$  is the 2 for corner columns

$$v_c = 0.4 \lambda \phi_c \sqrt{f'_c} \quad (8)$$

The British Code BS 8110-97 design equation is:

$$v = \frac{V}{ud} \leq v_c \quad (9)$$

Where:

$v$  is the design shear stress

$V$  is the shear force due to factored loads

$u$  is the perimeter at  $1.5d$  from the column face

$d$  is the effective depth of the slab

$v_c$  is the concrete shear stress resistance and can be calculated as follows:

$$v_c = \frac{0.79 k_1 k_2}{\gamma_m} \sqrt[3]{\frac{100 A_s}{ud}} \sqrt[4]{\frac{400}{d}} \quad (10)$$

Where:

$k_1$  is the enhancement factor for support compression, and is conservatively taken as 1.

$$k_2 = \sqrt[3]{\frac{f_{cu}}{25}} \quad , \quad 1 \leq k_2 \leq \sqrt[3]{\frac{40}{25}} \quad (11)$$

$\gamma_m$  is the partial safety factor of value 1.25

$f_{cu}$  is the characteristic cube concrete strength

$A_s$  is the effective steel area passing the perimeter of the critical section and should not be taken greater than  $0.03ud$ .

The critical section is located at  $1.5d$  from the face of the column or loaded area. The shear stress obtained at location  $1.5d$  is influenced by strength of concrete, size effect, and ratio of flexural reinforcement.

When gravity load, wind, earthquake, or other lateral loads cause transfer of unbalanced moment  $M$  between a slab and a column, the code increases the shear stress according to the following equation:

$$v_{\max} = \frac{V_{\text{eff}}}{ud} \leq v_c \quad (12)$$

Where:

$V_{\text{eff}}$  is the effective shear force and has different equations according to the column

position into building as follows:

1) For interior columns:

$$V_{eff} = V + \frac{1.5M}{x} \quad (13)$$

Where:

$x$  is the the side length of the perimeter considered parallel to bending axis

In the absence of calculations into braced structures with approximately equal spans, the code gives the following equation:

$$V_{eff} = 1.15V \quad (14)$$

Where,  $V$  is calculated on the assumption that the maximum design load is applied to all panels adjacent to the column considered.

2) For edge and corner columns:

$$V_{eff} = 1.25V + \frac{1.5M}{x} \quad (15)$$

In the absence of calculations into braced structures with approximately equal spans, the code gives the following equation:

$$V_{eff} = 1.4V \quad (16)$$

The European CEB-FIP Model Code 90 stated that the critical section is located at  $2d$  from the face of the column or loaded area. The conservative concrete shear resistance equation is limited by the value of the following equation (S.I. units):

$$v_c = 0.12k(100\rho f_c')^{1/3} \quad (17)$$

Where:

$$k = \text{size factor} = 1 + (200/d)^{1/2} \leq 2, \text{ d in mm} \quad (18)$$

$$\rho = \text{flexural reinforcement ratio} = (\rho_x \rho_y)^{1/2} \quad (19)$$

## 2. OBJECTIVES AND SCOPE OF STUDY

The main objectives of this study can be divided into the following points:

1. Applying the proposed finite element model on some of chosen tested slab-column connections that were done by some researchers [El-Salakawy et. al (1998); specimens XXX and HXXX].
2. Studying the effect of concrete compressive strength on the punching shear strength using ANSYS and codes.
3. Showing the impact of eccentricity to slab thickness ratio ( $e/t_s$ ) the punching shear strength using ANSYS and codes.
4. Representing the effect of column dimension to slab thickness ratio ( $b/t_s$ ) on the punching shear strength using ANSYS and codes.

In order to verify the finite element program for simulating the behavior of column-slab connections under gravity loads plus unbalanced moments, two models (see Table 1: Description of the analyzed specimens and Fig. 1) are based on two experimental work specimens [El-Salakawy et. al (1998); specimens XXX and HXXX] are applied.

Table 1 Description of the analyzed specimens

model	Slab reinforcement (RFT)		column vertical RFT area (mm <sup>2</sup> )	Slab dimensions (mm)			upper or lower column dimensions (mm)		
	Tension RFT area (mm <sup>2</sup> )	Compression RFT area (mm <sup>2</sup> )							
XXX	100	38	2946	1020	1540	120	250	250	700
HXXX	100	38	2946	1020	1540	120	250	250	700

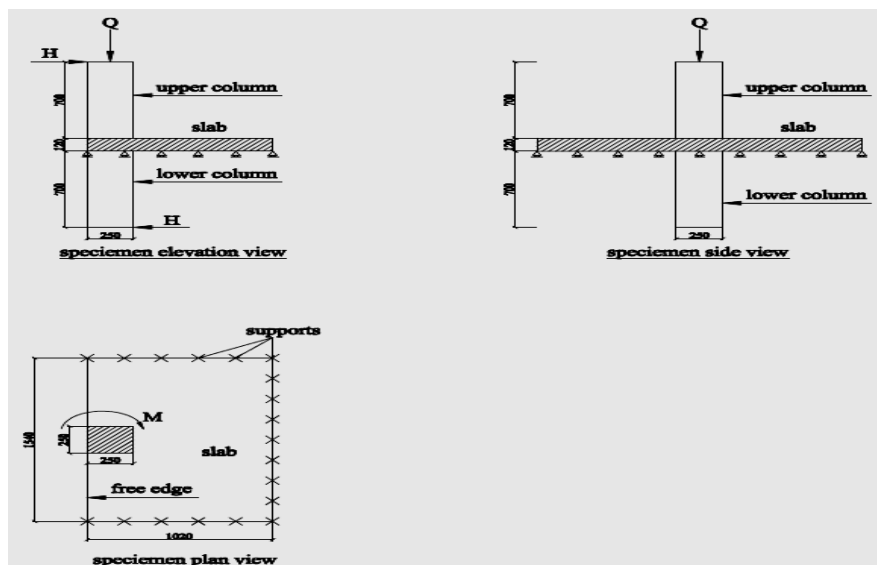


Fig. 1 Model dimensions (XXX, HXXX) (mm)

These objectives are fulfilled by analyzing 21 series of slab-column connections, as detailed in Table 2 and Figs. from 2 to 4, using the ANSYS software package. The results discussed include cracking and failure loads due to upper column loading. ANSYS was taken to test models under gravity loads (Q) plus unbalanced moments. Unbalanced moments (M) produced by applying horizontal forces H at the upper and lower columns in opposite direction, so the eccentricity will be calculated as  $e = M/Q$ , i.e. the unbalanced moment equals  $M = HxL$ , where  $L=1.6$  m for all model series. The slabs boundary conditions for the vertical translations of all joints were restrained; corner joints were fully restrained in the three directions.

Table 2 Summary of analyzed slab-column connections' features and variables (see Fig. 2 for geometric configuration)

position	Series	Constant/Variable Controlling Data and Their Ranges								e (mm)
		Slab Size(m) $L_x L_y t_s$	Column Size (cm)* bxb	Material property(MPa)			Reinforcement ratio			
				$f_{cu}$	$f_t$	$f_y$	Slab		Column VI.	
							Top	Bottom		
Interior Slab- Column Connection	A	1.60x1.60x0.2	25x25	25	2.5	360	0.56	0.56	1.63	0
	B		25x25	30	3.0	360	0.56	0.56	1.63	0
	C		25x25	35	3.5	360	0.56	0.56	1.63	0
	D		25x25	25	2.5	360	0.56	0.56	1.63	80
	E		25x25	25	2.5	360	0.56	0.56	1.63	500
	F		25x25	25	2.5	360	0.56	0.56	1.63	1000
	G	1.8x1.8x0.2	40x40	25	2.5	360	1.10	1.10	2.03	0
Edge Slab-Column Connection	H	1.6x0.9x0.2	25x25	25	2.5	360	1.10	1.10	1.63	0
	I		25x25	30	3.0	360	1.10	1.10	1.63	0
	J		25x25	35	3.5	360	1.10	1.10	1.63	0
	K		25x25	25	2.5	360	1.10	1.10	1.63	200
	L		25x25	25	2.5	360	1.10	1.10	1.63	500
	M		25x25	25	2.5	360	1.10	1.10	1.63	1000
	N	1.8x1.1x0.2	40x40	25	2.5	360	1.10	1.10	2.03	0
Corner Slab- Column Connection	O	0.9x0.9x0.2	25x25	25	2.5	360	1.10	1.10	1.63	0
	P		25x25	30	3.0	360	1.10	1.10	1.63	0
	Q		25x25	35	3.5	360	1.10	1.10	1.63	0
	R		25x25	25	2.5	360	1.10	1.10	1.63	250
	S		25x25	25	2.5	360	1.10	1.10	1.63	500
	T		25x25	25	2.5	360	1.10	1.10	1.63	1000
	U	1.1x1.1x0.2	40x40	25	2.5	360	1.10	1.10	2.03	0

Notes:

\* Upper or lower columns have constant height of 700 mm measured from slab surface.  
 RFT = steel reinforcement; Bott. = bottom RFT; VI. = vertical RFT; Hz. =horizontal RFT;  
 e = load eccentricity

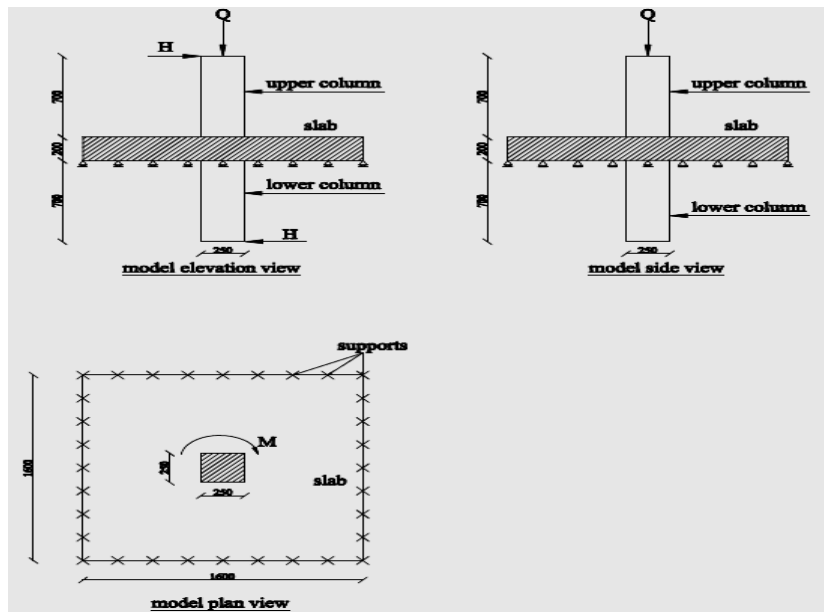


Fig. 2 Interior model dimensions (mm)

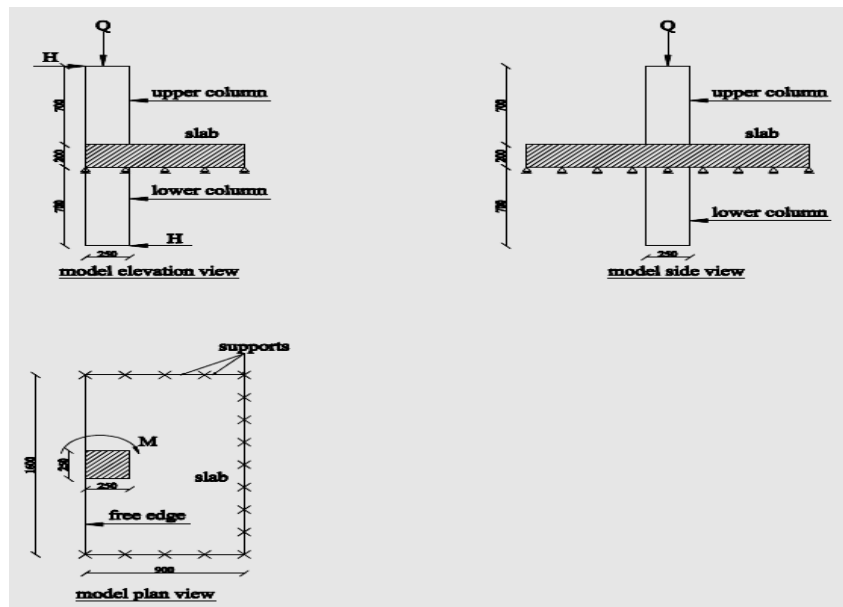


Fig. 3 Edge model dimensions (mm)

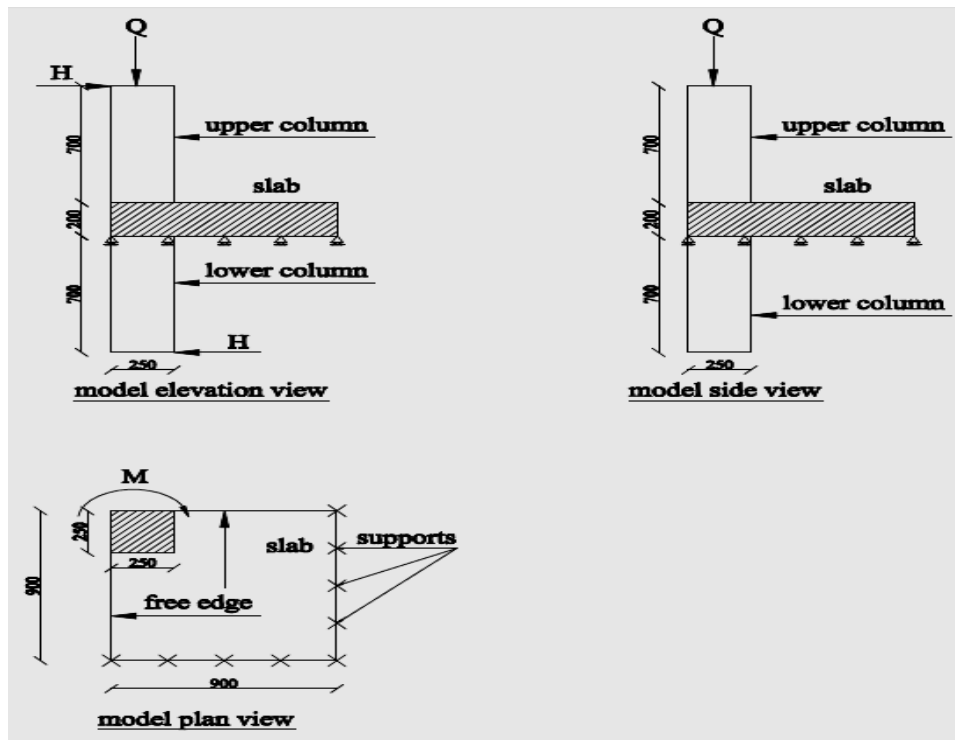


Fig. 4 Corner model dimensions (mm)

### 3. DEVELOPMENT OF STRUCTURAL MODELS USING ANSYS

#### 3.1 Material Properties

Concrete is modeled as a multi-linear isotropic material with a characteristic cubic compressive strength  $f_{cu} = 25, 30, \text{ and } 35 \text{ MPa}$  ( $f_c' = 20, 24, \text{ and } 28 \text{ MPa}$ ), an initial modulus of elasticity  $E_c = 22,000, 24,100, \text{ and } 26,030 \text{ MPa}$ , a flexure tensile strength  $f_{ctr} = 2.5, 3, \text{ and } 3.5 \text{ MPa}$ , and a Poisson's ratio  $\nu = 0.2$  using the eight-node solid element SOLID65. Further, the steel reinforcement is assumed to be an elastic-perfectly plastic material with identical behaviors in tension and compression. The elastic modulus for steel and its Poisson's ratio are taken  $200,000 \text{ MPa}$  and  $0.3$ , respectively. LINK180, a three-dimensional spar element with plasticity is employed to model the slab reinforcement. The yield strength of steel used for stirrups and longitudinal reinforcement is equal to  $240 \text{ MPa}$  and  $360 \text{ MPa}$ , respectively.

For specimens XXX and HXXX, characteristic cubic compressive strength  $f_{cu} = 41.25 \text{ MPa}$  ( $f_c' = 33 \text{ MPa}$ ), an initial modulus of elasticity  $E_c = 26999.44 \text{ MPa}$ , a flexure tensile strength  $f_{ctr} = 2.70 \text{ MPa}$ , and a Poisson's ratio  $\nu = 0.2$  using the eight-node solid element SOLID65. Further, the steel reinforcement is assumed to be an elastic-perfectly plastic material with identical behaviors in tension and compression. The elastic modulus for steel are taken  $1.8 \times 10^5$  for stirrups and  $1.95 \times 10^5 \text{ MPa}$  for main steel and its Poisson's ratio  $0.3$ . LINK180, a three-dimensional spar element with plasticity is

employed to model the slab reinforcement. The yield strength of steel used for both stirrups and longitudinal reinforcement are equal to 430 MPa and 545 MPa, respectively.

### 3.2 Loading and Boundary Conditions

The single vertical concentrated load is simulated by a series of point loads on all nodes located at the top of the upper column. The single horizontal concentrated load is simulated by a series of point loads on all nodes located at the top of the upper column and the bottom of the lower column in the opposite direction.

### 3.3 Meshing

A convergence study was carried out to determine an appropriate mesh density. Various mesh sizes were examined in ANSYS. The mesh was selected in a way that the nodes of solid elements representing concrete match with those of bar elements simulating the reinforcement. Full bond is assumed between concrete and reinforcement Fig. 5 shows the mesh of a typical slab-column connection.

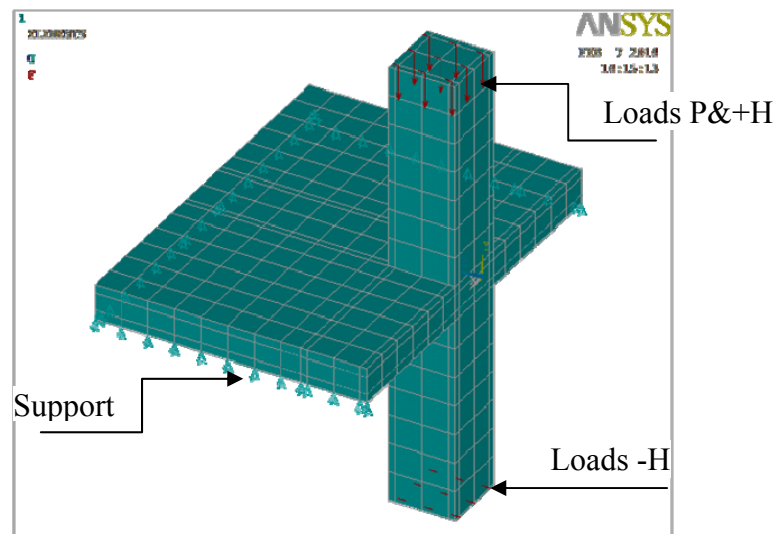


Fig. 5 Typical edge slab-column connection meshing

## 4. RESULTS AND DISCUSSIONS

### 4.1 Cracking and Failure Loads

The values of cracking and failure loads from finite element analysis of RC analyzed slab-column connection in series (A to U) are presented in Table 3.

Table 3 Cracking and failure loads of the analyzed slab-column connections in series (A - U)

series	slab-column connection	Cracking load (kN)	Failure load (kN)
A	Interior	110	510.00
B		120	560.00
C		130	670.00
D		70	392.50
E		40	175.00
F		20	75.00
G		110	618.75
H	Edge	75	358.92
I		80	370.69
J		85	439.81
K		60	382.66
L		40	145.13
M		20	65.00
N		100	390.5
O	Corner	15	210.64
P		20	249.66
Q		22.5	261.63
R		40	180.00
S		20	157.50
T		10	59.00
U		50	245.00

#### 4.1.1 Effect of cubic compressive strength of $f_{cu}$

To study the effect of concrete compressive strength on punching shear resistance of column slab connections, nine models of interior, edge, and corner slab-column connections with different  $f_{cu}$  were studied using ANSYS. Other parameters such as  $f_y$ ,  $f_t$ , slab dimensions, and tension steel ratio were constants for all modeled connections. The boundary conditions and method of loading were as per as mentioned above. Models dimensions and material properties are listed in Table 2. Also, cracking load and failure loads are listed in Table 3. From this result, it can be noticed that the change in punching shear resistance is slightly affected by changing concrete compressive strength.

#### 4.1.2 Effect of eccentricity to slab thickness ratio ( $e/t_s$ )

To study the effect of eccentricity to slab thickness ratio ( $e/t_s$ ) on punching shear resistance of column slab connections, three models of interior, edge, and corner slab-column connections with different ( $e/t_s$ ) were studied using ANSYS. Other parameters such as  $f_{cu}$ ,  $f_y$ ,  $f_t$ , slab dimensions, and tension steel ratio were constants for all modeled connections. The boundary conditions and method of loading were as per as mentioned above. Models dimensions and material properties are listed in Table 2.

Also, cracking load and failure loads are listed in Table 3. From this result, it can be noticed that the change in punching shear resistance is highly affected by eccentricity to slab thickness ratio ( $e/t_s$ ).

#### 4.1.3 Effect of column dimension to slab thickness ratio ( $b/t_s$ )

To study the effect of column dimension parallel to analysis direction to slab thickness ratio ( $b/t_s$ ) on punching shear resistance of column slab connections, three models of interior, edge, and corner slab-column connections with different ( $b/t_s$ ) were studied using ANSYS. Other parameters such as  $f_{cu}$ ,  $f_y$ ,  $f_t$ , slab dimensions, and tension steel ratio were constants for all modeled connections. The boundary conditions and method of loading were as per as mentioned above. Models dimensions and material properties are listed in Table 2. Also, cracking load and failure loads are listed in Table 3. From this result, it can be noticed that the change in punching shear resistance is highly affected by column dimension parallel to analysis direction to slab thickness ratio ( $b/t_s$ ).

Tables from 4 to 6 show the increasing in punching resistance by applying different parameters mentioned before according to some of chosen codes and ANSYS.

Table 4 Comparison between maximum punching forces (kN) predicted by different codes and ANSYS for series (A to G)

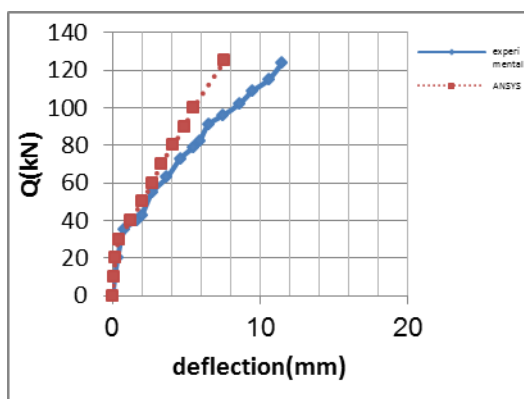
code	Maximum punching forces(kN) for series						
	(A)	(B)	(C)	(D)	(E)	(F)	(G)
ACI 318-08	373.07	408.67	441.42	236.46	121.21	80.12	445.03
BS 8110-97	419.86	446.17	469.70	361.62	209.23	139.33	504.40
CEP-FIP MC 90	429.27	456.17	480.21	371.75	218.24	146.31	513.08
ANSYS	510.00	560.00	670.00	392.50	175.00	75.00	618.75

Table 5 Comparison between maximum punching forces (kN) predicted by different codes and ANSYS for series (H to N)

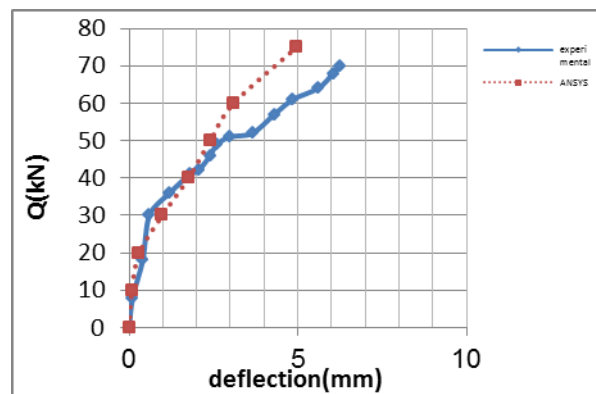
code	Maximum punching forces(kN) for series						
	(H)	(I)	(J)	(K)	(L)	(M)	(N)
ACI 318-08	242.78	265.94	287.24	117.23	81.64	51.13	343.93
BS 8110-97	245.16	260.52	274.25	174.78	122.17	81.36	308.56
CEP-FIP MC 90	249.56	265.19	279.17	214.64	214.64	214.64	312.41
ANSYS	358.92	370.69	439.81	382.66	145.13	65.00	390.50

Table 6 Comparison between maximum punching forces (kN) predicted by different codes and ANSYS for series (O to P)

code	Maximum punching forces(kN) for series						
	(O)	(P)	(Q)	(R)	(S)	(T)	(U)
ACI 318-08	149.47	163.75	176.87	74.19	52.13	33.45	216.92
BS 8110-97	140.19	148.97	156.83	63.95	55.91	34.92	182.46
CEP-FIP MC 90	142.23	151.14	159.12	107.31	107.31	107.31	184.14
ANSYS	210.64	249.66	261.63	180.00	157.50	59.00	245.00



XXX



HXXX

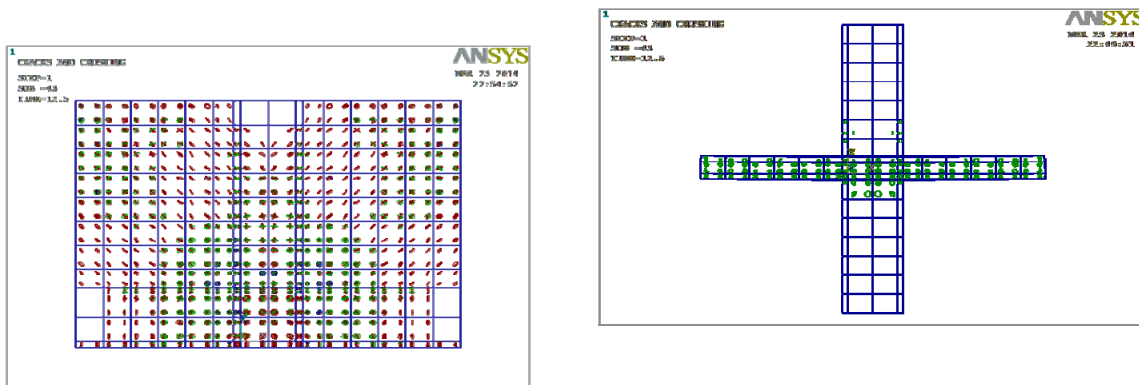
Fig. 6 Load deflection curve comparison for specimen (XXX and HXXX) by experimental results and ANSYS

For specimens XXX and HXXX, the load-deflection curves can be obtained directly from program as shown in the following figures.

#### 4.2 Crack Patterns and Mode of Failure

##### 4.2.1 Crack Patterns

All models were failed in a brittle punching mode. The formation of flexural cracks on the tension face of the slab was initiated at a specified vertical load of about 20% to 25% of the total failure load for interior models and about 15% to 20% for exterior models. The cracks first started at the inner corners of the column and developed towards the supports and then developed over entire slab. The flexural cracks reached the simply supported edges of the model at vertical load of about 50% of the total failure load for interior models and about 30% to 40% for exterior models. The inclined cracks around the column initiated at failure load and extended up to top compression zone within the slab to make punching failure surface. Fig. 7 shows crack patterns at failure for edge slab-column connection.



(a) plan view

(b) side view

Fig. 7 Crack patterns at failure for edge slab-column connection

#### 4.2.2 Mode of Failure

For interior and exterior slab-column connection, referring to Fig. 8 and Fig. 9 respectively, all models were failed in a brittle punching mode. The formation of flexural cracks on the tension face of the slab was initiated first. The cracks started at the inner corners of the column and developed for interior models towards the supports, but developed for exterior models towards the free edge and then developed over entire slab. The inclined cracks around the column initiated at failure load and extended up to top compression zone within the slab to make punching failure surface.

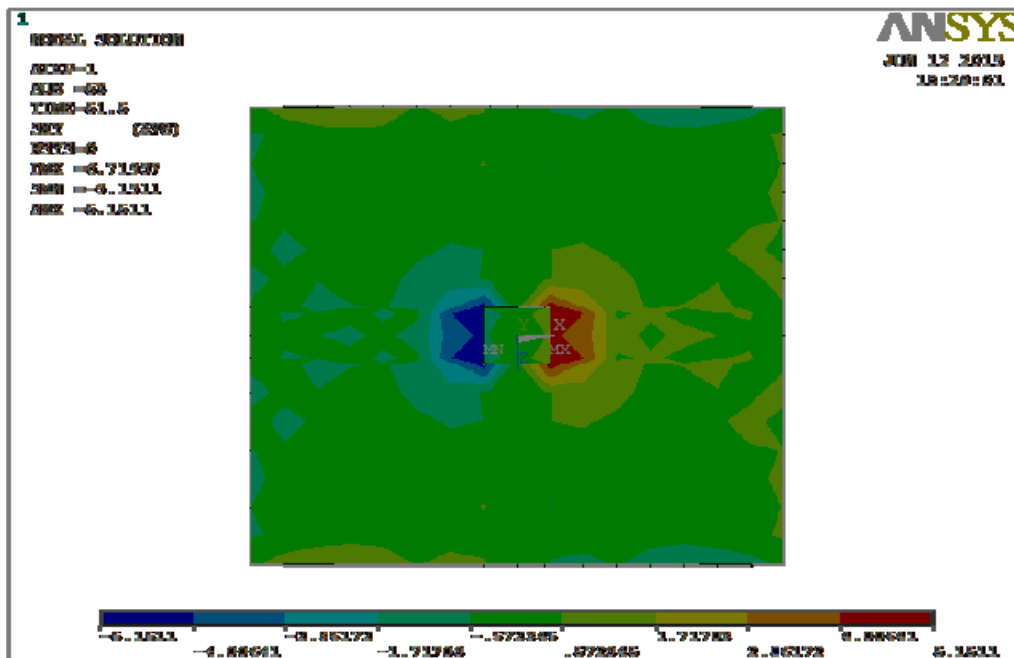


Fig. 8 Nodal SXY stresses of interior slab-column connection

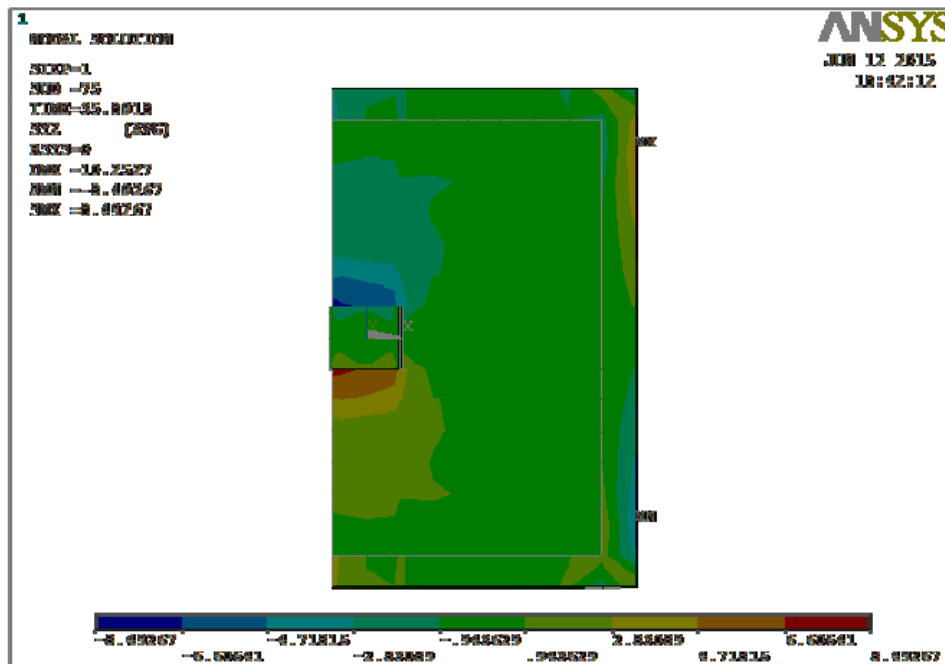


Fig. 9 Nodal SZY stresses of exterior slab-column connection

## 5. CONCLUSIONS

Based on the evaluation of published results of the previous researches as well as the numerical analysis of results obtained from finite element modeling of reinforced concrete slab-column connections, several conclusions are illustrated below.

- FEM results provided good agreement with the available experimental results of the ultimate load and associated deflection.
- Column dimension to slab thickness ( $b/t_s$ ) approximately had also a major effect on punching resistance, but the ACI standard underestimates the strength of interior, edge, and corner slabs by approximately 28%, 12%, and 11% respectively, compared with FEM results.
- Generally, the difference of the punching shear force in slabs calculated applying ACI 318-05, CEP-FIP MC 90, and BS 8110-97 methods from the punching shear force in slabs obtained numerically is statistically significant. This shows that none of the analyzed methods allows an accurate calculation of punching shear force.
- For slab-column connections subjected to high eccentricity, it is not recommended to use any simplified method mentioned in any code for calculating punching shear stresses, and a detailed method, or a special finite element analysis has to be used.

- Prevention of punching failure of column-slab connections transferring moments depends on the accuracy of the FEM model or the accuracy of the calculations of shear stresses produced by moment transfer.

## REFERENCES

- Younis, G.S., (2015), "Finite element estimates of punching shear strength", M. Sc. Thesis, Dept. of Structural Eng., Cairo University, Cairo, Egypt.
- Megally, S. and Ghali, A., (2000), "Punching of concrete slabs due to column moment transfer", *J. Struct. Eng., ASCE*, 126(2) 180-188.
- Mufti, A.A. and Hassan, T.K., (2005), "Finite element analysis and theoretical study of punching shear strength of concrete bridge decks", *Canadian Journal of Civil Engineering*, 32(2) 449 -453.
- Polak, M.A., (2005), "Ductility of Reinforced concrete flat slab-column connections", *Computer-Aided Civil and Infrastructure Engineering*, 20 184-193.
- Hong-Gun Park, Kyoung-Kyu Choi, (2007), "Strength of exterior slab-column connections subjected to unbalanced moments", *Engineering Structures* 29 1096-1114.
- Choi, K.K., Taha, M.R., and Sherif, A.G., (2007), "Simplified punching shear design method for slab-column connections using fuzzy learning", *ACI Structural Journal*, 104(4) 438–447.
- Wang, W. and Teng, S., (2008), "Finite –Element Analysis of Reinforced Concrete Flat Plate Structures by Layered Shell Element", *Journal of Structural Engineering ASCE*, 134 1862-1872.
- Guan, H., (2009), "Prediction of punching shear failure behavior of slab-edge column connections with varying Opening and column parameters", *Advances in structural engineering*, 12(1), 19-36.
- Ruiz, M.F. and Muttoni, A., (2009), "Applications of critical shear crack Theory to Reinforced Concrete Slab with transverse Reinforcement", *ACI Structural Journal*, 106(4) 485-494.
- Thomas, H.K., Kang, J.W., and Elwood, K.J., (2009), "Nonlinear Modeling of Flat-Plate systems", *Journal of Structural Engineering ASCE*, 135 147-158.
- ACI Committee 318, (2005), "Building Code Requirements for Structural Concrete (ACI 318-05)", USA.
- ACI-ASCE Committee 426 on shear and Diagonal Tension, (1974), "The Shear Strength of Reinforced Concrete Members-Slabs", *Journal of the Structural Division, Proceedings of ASCE*, 100 1543-1591.
- BS 8110, (1997), "Structural Use of Concrete, Part 1: Code of Practice for Design and Construction", British Standards Institute, London, UK.
- CSA-A23.3-04, (2004), "Design of Concrete Structures for Buildings", Canadian Standard Association, Mississauga, Canada.
- El-Salakawy, E.F., Polak, M.A., and Soliman, M.H., (1998), "Slab-column edge connections subjected to high moments", *Canadian Journal of Civil Engineering*, 25(3) 526-538.